

# Cu 도핑된 ZnO 나노로드의 전기적 특성

## Electrical characteristics of Cu-doped ZnO nanorods

\*R. Mohan<sup>1</sup>, S. Saini<sup>2</sup> and #S. J. Kim( kimsangi@jejunu.ac.kr)<sup>1</sup>

<sup>1</sup>Department of Mechatronics Engineering and <sup>2</sup>Department of Mechanical Engineering, Jeju National University, Jeju 690-756, Korea

Key words : Cu-doped ZnO, nanowires, focused-ion beam lithography

### 1. Introduction

Zinc oxide has a number of advantages, such as high resistance to radiation damage, high breakdown strength and temperature stability, low cost and simplicity of device fabrication [1]. In recent years, ZnO has attracted extensive attention for its potential in blue- and UV-emitting optoelectronics applications [2-4]. So far ZnO based optoelectronic devices were based on n-type ZnO wires due to the unavailability of p-type wires. However, the growth of p-type conducting ZnO wires is the greatest challenge and the prerequisite of nano p-n junctions as the base structure of oxide electronic and optoelectronic devices. Achieving high-quality p-type ZnO has been a major challenge for the fabrication of long-lasting and robust electro-optic devices. Nitrogen, arsenic, phosphorus and antimony have been the promising anionic dopants for the p-type conductivity in ZnO. Nevertheless, p-type doping of ZnO using group V elements, such as P, As, Sb, and Bi has been reported recently [5-8]. In contrast to numerous attempts to p-type doping performed on ZnO films, there are only few reports on acceptor-doped ZnO wires for p-type conductivity, partially due to the difficulties of preparation and electrical characterizations of single wires. A potential p-type doping candidate for ZnO is Cu. Cu, as a group I(b) element (Cu, Ag and Au), can assume a valence of either +1 or +2 depending on its chemical configuration, for example in the compounds Cu<sub>2</sub>O and CuO, respectively. The radii of Cu<sup>+</sup> (0.06 nm) and Cu<sup>2+</sup> (0.057 nm) ions are similar to that of Zn<sup>2+</sup> ion (0.06 nm) [9]. Cu significantly affects the electrical, chemical, structural and optical properties of ZnO, and the study of the electronic state of Cu in ZnO has been the subject of interest for a long time [10-12].

In this letter, we report the preparation of Cu-doped ZnO by vapor transport growth method. Single nanorod device was fabricated using FIB technique. The low temperature electrical characteristics were presented

### 2. Experimental Procedure

Vapor transport technique was used for the growth of Cu doped ZnO nanorods. The schematic of the experimental setup for growth of Cu doped ZnO is shown in Fig.1. In this technique, a horizontal quartz tube furnace was used. A mixture of ZnO, graphite, Zn, and CuCl<sub>2</sub> in 1: 1: 0.5: 0.05 ratio (by weight) was used as source material. It was loaded in an alumina boat and placed in the center of 1 meter long quartz tube. High purity argon gas was introduced through one side of the quartz tube, while the other side was connected to a water bubbler. The source material was heated to 1100 °C at 360 °C/h rate under a constant argon flow of 250 sccm. When the temperature reaches 800 °C, oxygen gas is also introduced with a flow rate of 35 sccm. The furnace was maintained under these conditions for 1 h and then cooled to room temperature at a rate of 6 °C/min. The nanorods were collected at 20 cm away from the source in up flow direction of gas flow. The cross-sectional diameter and average length of whiskers are 10 μm and 5 mm respectively.

X-ray diffraction patterns of synthesized samples were recorded with a Rigaku D/MAX 2200H diffractometer system with CuKα irradiation (λ=1.5418 Å). Morphologies of the synthesized ZnO nanostructures were observed by a field emission scanning electron microscope (FE-SEM, JEOL, JSM-6700F). For the device fabrication, silver is deposited for electrode on a MgO 100 substrate using a shadow mask through thermal evaporation method. The structure of the shadow mask is shown in Fig. 2(a). A 3 μm

separation was made through focused ion beam (FIB) etching technique. Though dielectrophoresis method the Cu-doped ZnO nanorods were aligned on the metal electrode. The two ends of a single nanorod were fixed with W using FIB deposition technique. The different fabrication steps were shown in the Fig. 2. The electrical transport measurements were done in Keithley 2400 source-meter and 2182A nanovoltmeter, which were interfaced with LABVIEW program. A closed-cycle refrigerator was used for the low temperature transport measurements.



Fig. 1 Experimental setup for growth of Cu doped ZnO nanorods.

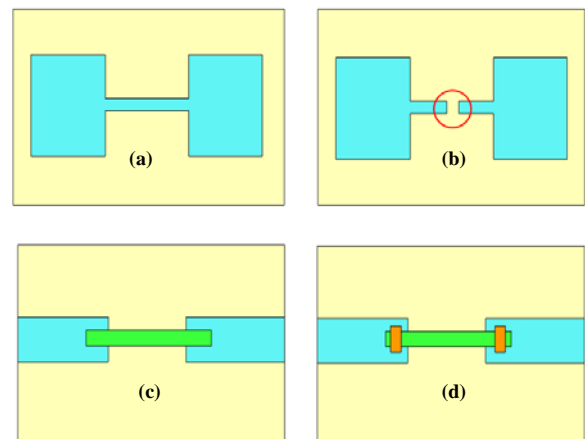


Fig. 2 Device fabrication steps, (a) Deposition of Silver using shadow mask; (b) FIB etching for making 3μm separation between two silver electrodes; (c) Aligning Cu-doped nanorods on two silver electrodes using dielectrophoresis technique; (d) Fixing Cu-doped nanorods on silver electrode with W using FIB deposition. (c) and (d) are magnified area of Fig. (b) shown by red circle.

### 3. Results and Discussion

The XRD patterns of the pure and Cu-doped ZnO nanorods are illustrated in Fig. 3(a). The diffraction peaks were indexed with the Powder Diffraction Standards data (JCPDS 3-1457), showing that the main structure of the samples is the wurtzite structure of ZnO. Only peaks corresponding to ZnO wurtzite phase were found in the XRD patterns of the undoped and Cu doped samples. The absence of Cu related peaks rules out the existence of Cu-based clusters within the detection limit of XRD. There is a slight shift in XRD peaks towards the higher angle with the Cu doping compared to the undoped ZnO. This shift is attributed to the shrinkage of ZnO crystal lattice due to the

substitution of  $Zn^{2+}$  (0.06 nm) by smaller  $Cu^{2+}$  (0.057 nm) [9]. This observation shows the doping of Cu in ZnO crystal lattice. The FESEM images of the prepared undoped and Cu doped sample are shown in Fig. 3(b). These images show that the undoped ZnO have nanoneedle like morphology. Whereas Cu doped ZnO have nanorods morphology. The Cu doped nanorods have diameter of ~ 60-90 nm and length of 1.5 -3  $\mu m$  respectively.

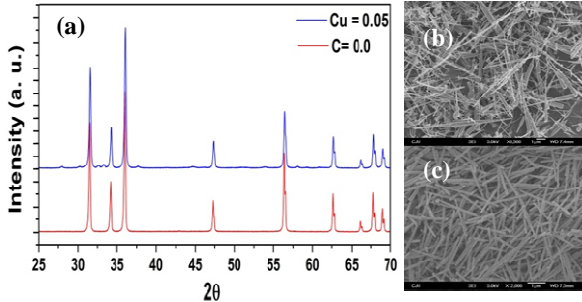


Fig. 3 (a) XRD pattern showing single phase ZnO structure (b) and (c) FESEM image of undoped and Cu-doped ZnO respectively.

The FIB fabricated device of Cu-doped ZnO nanorod is shown in Fig.4.

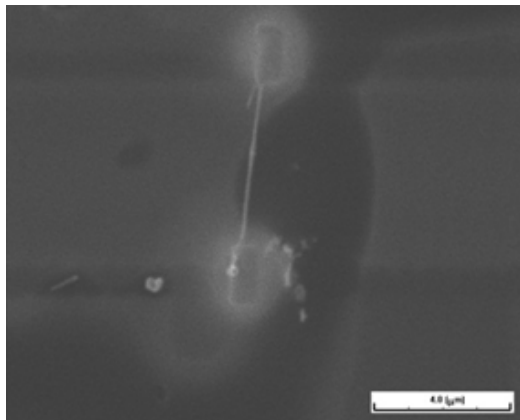


Fig. 4 Device fabricated using single Cu-doped ZnO nanorod. The individual nanorod is fixed on silver electrode using FIB deposition of W.

The fabricated device is used to study the electrical characteristics at low temperature. Low temperature electrical resistance vs. temperature (R-T) behavior of single Cu-doped ZnO nanorod in the temperature range 10-300 K is shown in the Fig. 5(a).

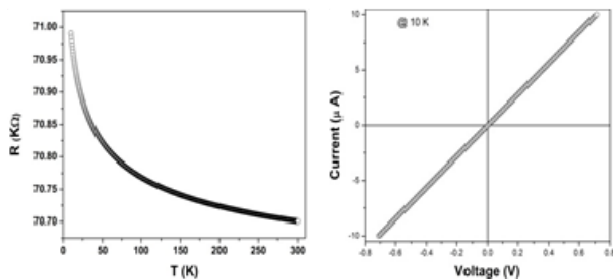


Fig. 5 (a) Low temperature electrical resistance vs. temperature (R-T) behavior of single Cu-doped ZnO nanorod; (b) Current (I)- voltage (V) characteristics of the device.

The semiconducting behavior of Cu-doped ZnO nanorod is clearly evident from this figure. This R-T behavior can be easily explained on the basis of variable range hopping (VRH) mechanism. The I-V curve at 10 K shows ohmic behavior. The detail investigation of the fabrication devices is in progress.

#### 4. Conclusion

Cu-doped ZnO nanowires with an average diameter of 60-90 nm have been synthesized by a vapor transport method. Thermal evaporation is used for fabricating silver electrodes. Focused ion beam etching and deposition technique was used to fix a single Cu-doped ZnO nanorod on the silver electrode. The Low temperature R-T of single nanorod show semiconducting behavior. Current-voltage characteristics at 10K show ohmic behavior.

#### Acknowledgment

This work was supported by National Research Foundation of Korea Grant (2009-0087091). A part of this research was supported by 2000 Jeju Sea Grant College Program funded by Ministry of Land, Transport and Maritime Affairs (ML TM), Republic of Korea.

#### References

1. B D Yuhas, D O Zitoun, P J Pauzauskie, R R He and P D Yang, *Angew. Chem. Int. Edn* **45**, 420-3, 2006
2. D.C. Look, D.C. Reynolds, J.R. Sizelove, R.L. Jones, C.W. Litton, G. Cantwell, W.C. Harsch, *Solid State Commun.* **105**, 399, 1998.
3. S.J. Pearton, D.P. Norton, K. Ip, Y.W. Heo, T. Steiner, *J. Vac. Sci. Technol. B* **22**, 932, 2004.
4. J.M. Bian, X.M. Li, X.D. Gao, W.D. Yu, L.D. Chen, *Appl. Phys. Lett.* **84**, 541, 2004.
5. B. Xiang, P. W. Wang, X. Z. Zhang, S. A. Dayeh, D P R Aplin, C Soci, D P Yu and D L Wang *Nano Lett.* **7**, 323-8, 2007.
6. M. P Lu, J Song, M Y Lu, M T Chen, Y Gao, L J Chen and Z.L. Wang, *Nano Lett.* **9** 1223-7, 2009
7. S. Limpijumngong, S B Zhang, S H Wei and C H Park, *Phys. Rev. Lett.* **92**, 155504, 2004
8. U. Wahl, J.G. Correia, T. Mendonca and S. Decoster, *Appl. Phys. Lett.* **94**, 215503, 2009.
9. R. D. Shannon *Acta Cryst.* **A32**, 751-767, 1976.
10. R. C. Wang, C. P. Liu, J. L. Huang, and S. J. Chen, *Appl. Phys. Lett.* **88**, 023111-023113, 2006
11. P. Fons, A. Yamada, K. Iwata, K. Matsubara, S. Niki, K. Nakahara, H. Takasu, *Nucl. Instrum. Methods Phys. Res. B*, **199**, 190, 2003.
12. G. H. Kim, D.L. Kim, B.D. Ahn, S.Y. Lee, H.J. Kim, *Microelectronics Journal*, **40**, 272-275, 2009